SCIENTIFIC REPORTS
nature research

OPEN

# Peculiarities of pseudogap in $Y_{0.95}Pr_{0.05}Ba_2Cu_3O_{7-\delta}$ single crystals under pressure up to 1.7 GPa

A. L. Solovjov[1], L. V. Omelchenko[1], E. V. Petrenko[1], R. V. Vovk[2], V. V. Khotkevych[3] & A. Chroneos[4,5*]

**The effect of hydrostatic pressure up to P = 1.7 GPa on the fluctuation conductivity σ′(T) and pseudogap Δ*(T) in $Y_{0.95}Pr_{0.05}Ba_2Cu_3O_{7-\delta}$ single crystal with critical temperature $T_c$ = 85.2 K (at P = 0) was investigated. The application of pressure leads to the increase in $T_c$ with $dT_c/dP = +1.82\ K{\cdot}GPa^{-1}$ while the resistance decreases as $d\ln\rho(100\ K)/dP = -(10.5 \pm 0.2)\ \%{\cdot}GPa^{-1}$. Regardless of the pressure, in the temperature interval from $T_c$ to $T_0$ (~88 K at P = 0) the behaviour of σ′(T) is well described by the Aslamazov – Larkin (AL – 3D) fluctuation theory, and above the $T_0$ by the Lawrence – Doniach theory (LD). The Maki-Thompson (MT – 2D) fluctuation contribution is not observed. This indicates the presence of structural defects in the sample induced by Pr. Here it is determined for the first time that when the pressure is applied to the $Y_{1-x}Pr_xBa_2Cu_3O_{7-\delta}$ single crystal, the pseudogap increases as $d\ln\Delta^*/dP = 0.17\ GPa^{-1}$.**

The pseudogap (PG) state, which is realized in high-temperature superconductors (HTSCs) at the characteristic temperature T* » $T_c$ with the doping less than optimal, is one of the most mysterious properties of HTSC cuprates[1–9]. Understanding the physics of the PG would answer the question about the mechanism of superconducting pairing in HTSCs, which is also not fully clarified yet[3–7,10,11]. One of the most promising materials for studying the PG is the $YBa_2Cu_3O_{7-\delta}$ (YBCO) family. It is so due to the possibility of variation in its composition by substitution of yttrium (Y) with the isovalent analogues, or changing the degree of oxygen nonstoichiometry (see review[12] and references therein). The compounds $Y_{1-x}Pr_xBa_2Cu_3O_{7-\delta}$ (YPrBCO) with partial substitution of Y by praseodymium (Pr) atoms are of particular interest in that respect. The replacement of Y with other rare-earth elements in this compound does not lead to a significant change in its resistive characteristics[13]. The only exception is the replacement of Y with Pr (also known as the "praseodymium anomaly"), which leads to a noticeable increase in the resistivity ρ and a decrease in the critical temperature $T_c$ of the superconducting (SC) transition[14–18]. It is believed that in YPrBCO this occurs as a result of the interaction of holes with electrons of the 4 f shell of Pr. Finally, with increase in Pr content (regardless of the oxygen content), in $PrBa_2Cu_3O_{7-\delta}$ (PrBCO) the charge carriers are localized in the Ferenbacher-Rice energy zone (RF)[19]. Thus, PrBCO becomes a dielectric being isostructural to YBCO[16–18]. The PrBCO dielectric inclusions, arising in the process of manufacturing of YPrBCO crystals, form multiple defects in the YBCO superconducting matrix[15–18], which significantly affect the transport properties of the sample. Therefore, doping of the $Y_{1-x}Pr_xBa_2Cu_3O_{7-\delta}$ with Pr on the one hand leads to a gradual suppression of superconductivity with increasing of the concentration x, and on the other, it allows to preserve almost constant both the lattice parameters and the oxygen content (7-δ) of the sample under investigation[18–20]. It should also be stressed that $Pr^{+3}$ atoms have an intrinsic magnetic moment of $\mu_{Pr} \approx 3.58\mu_B$[21], which is $m_{eff} \approx 2\mu_B$ in the PrBCO compound[22]. That is why the study of the effect of Pr impurity on the properties of YPrBaCuO single crystals is considered very promising for revealing the mechanisms of the interplay of the superconductivity and magnetism in HTSC, (for example[23,24] and references given therein), which is important for the final clarification of the physical nature of both the PG and high-temperature superconductivity in general[1,2,5–7,10,11].

[1]B. Verkin Institute for Low Temperature Physics and Engineering, NAN of Ukraine, 47 Nauky Avenue, Kharkiv, 61103, Ukraine. [2]V. Karazin Kharkiv National University, 4 Svobody Square, Kharkiv, 61077, Ukraine. [3]Diamond Light Source Ltd., Harwell Science and Innovation Campus, Didcot, OX11 0DE, United Kingdom. [4]Department of Materials, Imperial College, London, SW7 2AZ, UK. [5]Faculty of Engineering, Environment and Computing, Coventry University, Priory Street, Coventry, CV1 5FB, United Kingdom. *email: alexander.chroneos@imperial.ac.uk

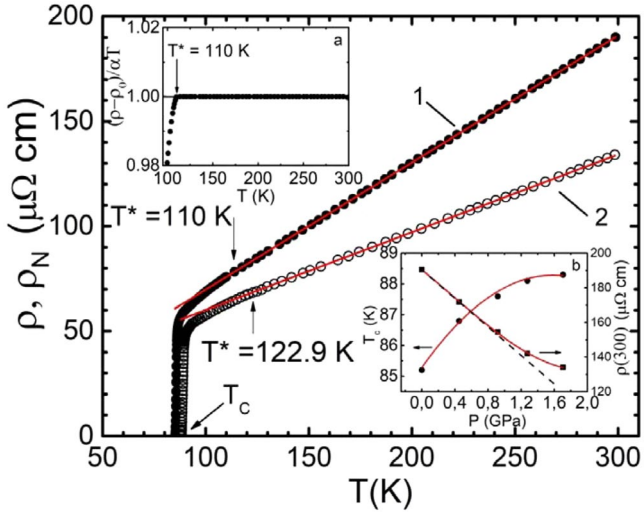


**Figure 1.** Temperature dependences of the resistivity ρ of $Y_{0.95}Pr_{0.05}Ba_2Cu_3O_{7-\delta}$ single crystal at P = 0 (curve 1, dots) and at P = 1.7 GPa (curve 2, circles). Straight dashed lines designate extrapolated $\rho_N(T)$. The inset (**a**) illustrates the method of determining T* with the use of the criterion $[\rho(T) - \rho_0)]/aT = 1$[45], insert (**b**) - pressure dependence of $T_c$ and ρ(300 K).

Hydrostatic pressure is an effective tool for studying HTSCs (refer to[12] and references therein), which enables validating the adequacy of numerous theoretical models, as well as establishing most significant parameters of HTSC structures, that determine their physical characteristics in normal and SC states.

In cuprates the $dT_c/dP$ dependence is mostly positive, while the derivative dlnρ/dT is negative and is relatively large[25–31]. However, the data given in studies of the effect of pressure on the $T_c$ of YPrBCO compounds (see, for example, Reviews[12,32]) are often inconsistent. The registration of both positive and negative baric derivative $dT_c/dP$ is reported, and in some cases the sign change of the $dT_c/dP$[12,32] takes place. Importantly, a significant part of the experimental data was obtained on ceramics, films, and textured samples of very different processing history[13–17,32]. In the case of single-crystal samples, difficulties may be caused by the appearance in the system of a sufficiently disordered structure of twin boundaries (TB)[33,34]. TB being extended two-dimensional defects can serve as drains for lower dimensionality defects, which in turn represent strong scattering centers for normal and fluctuation charge carriers[12,35], thereby having a significant impact on charge transfer processes in a particular experimental sample.

Notably, in the literature there are no experimental data on the effect of pressure in compounds with Pr concentration $x < 0.1$. It is the weakly Pr doped samples that demonstrate interesting phenomena of suppression of the pseudogap state and anomalous extension of the temperature range of the linear ρ(T) dependence[18,24,36]. When pressure is applied, the volume of the unit cell decreases contributing to the ordering of the system leading to a decrease in the number of structural defects and a decrease in ρ[12,28,37]. At any rate, the mechanisms of influence of pressure on both $T_c$ and ρ are not fully understood, as the nature of the transport properties of HTSC is not completely clear. The main contribution to the conductivity of cuprates is by the $CuO_2$ planes, between which there is a relatively weak interplanar interaction. It is assumed that the pressure leads to an increase in the density of charge carriers $n_f$ in the conducting $CuO_2$ planes and, as a result, to a decrease in ρ[12,28]. An increase in $n_f$ under pressure should also lead to an increase in $T_c$, i.e. to a positive $dT_c/dP$ value as observed in experiments[25,27,31,38,39]. Nevertheless, there are only very few studies that investigated the effect of pressure on the fluctuation conductivity and PG in HTSC cuprates[12,38,39], and, as far as we know, in the YPrBCO such studies have not been carried out at all.

In the present study we investigated the effect of hydrostatic pressure up to P = 1.7 GPa on resistive characteristics, the excess conductivity σ′(T) and the pseudogap Δ*(T) of doped with Pr ($x \approx 0.05$) single crystals of $Y_{1-x}Pr_xBa_2Cu_3O_{7-\delta}$ with nearly stoichiometric oxygen content. The geometry of the transport current I flow was chosen parallel to the TB (I || TB), which made it possible to minimize the effects of scattering on the twin boundaries[30,40].

## Results and Discussion

**Resistive characteristics.** Temperature dependences of the resistivity $\rho(T) = \rho_{ab}(T)$ of the $Y_{0.95}Pr_{0.05}Ba_2Cu_3O_{7-\delta}$ single crystal measured at atmospheric pressure (P = 0) (curve 1) and at P = 1.7 GPa (curve 2) are shown in Fig. 1. In this figure, the values of $T_c$ and ρ(300) at P = 0 were 85.2 K and 190 μΩ·cm, respectively. Thus, compared to the optimally doped (OD) pure YBaCuO single-crystal samples, the critical temperature after Pr doping dropped by 5–7 K, at the same time being accompanied by the 30–40 μΩ·cm increase in $\rho_{ab}(300)$, which is consistent with previous studies[12,25–29]. At all applied pressures, the dependences ρ(T) had the shape typical to OD HTSCs[39,41–44]. In the wide temperature range from T* to 300 K, the ρ(T) dependencies are linear with the slope $d\rho/dT \approx 0.61$ μΩ·cm/K (P = 0) and $d\rho/dT \approx 0.37$ μΩ·cm/K (P = 1.7 GPa). The slope was determined by approximating the experimental dependences ρ(T) by the straight line equation $\rho(T) = \rho_0 + aT$, where $a = d\rho/dT$ and $\rho_0$

| P (GPa) | ρ(300 K) μΩ(cm) | ρ(100 K) μΩ(cm) | $T_c$ (K) | $T_c^{mf}$ (K) | $T_G$ (K) | $T_o$ (K) | $T_{01}$ (K) | $\Delta T_{fl}$ (K) | $d_{01}$ (Å) | $\xi_c(0)$ (Å) |
|---|---|---|---|---|---|---|---|---|---|---|
| **0** | 190.05 | 69.22 | 85.2 | 85.85 | 85.97 | 88.0 | 92.77 | 6.8 | 6.43 | 1.84 |
| **0.45** | 171.84 | 67.41 | 86.8 | 87.51 | 87.66 | 90.18 | 96.72 | 9.06 | 6.35 | 2.03 |
| **0.92** | 154.42 | 65.10 | 87.6 | 88.42 | 88.58 | 91.32 | 98.78 | 10.2 | 6.3 | 2.12 |
| **1.27** | 142.0 | 61.84 | 88.1 | 88.77 | 88.92 | 91.72 | 99.18 | 10.26 | 6.22 | 2.14 |
| **1.70** | 134.0 | 57.94 | 89.1 | 89.17 | 89.4 | 92.15 | 99.53 | 10.13 | 6.22 | 2.16 |

**Table 1.** Changes in the parameters of the $Y_{0.95}Pr_{0.05}Ba_2Cu_3O_{7-\delta}$ single crystal under pressure.

is the residual resistance which is the intersection of this straight line with the Y axis at T = 0. The approximation confirmed high linearity of the dependencies with the root-mean-square error of 0.002 ± 0.001 in the specified T interval for all the samples studied. The deviation of ρ(T) from linearity towards smaller values determines the PG opening temperature T*. For the sake of accurate determination of T*, the criterion $(\rho(T) - \rho_0)/aT = 1$ was used[45], which is obtained by transforming the equation of the straight line. In this case, T* is defined as the deviation temperature of $(\rho(T) - \rho_0)/aT$ from 1, as shown at Fig. 1, box (a). In this case, the deviation from linearity is very sharp, which allows T* to be determined with great accuracy. In total five curves obtained at pressures P = 0, 0.45, 0.92, 1.27 and 1.7 GPa, which can be considered as 5 different samples (Y0 – Y5, respectively) were analysed. The corresponding resistive curves for intermediate pressures have a similar shape and are located between the ρ(T) curves at P = 0 and P = 1.7 GPa. They are not shown in Fig. 1 for clarity.

The temperature of the resistive transition to the SC state, $T_c$ (R = 0) was determined by extrapolation of the linear part of the SC transition towards the intersection with the temperature axis[25–27,38,39]. Notably, the width of resistive transitions $\Delta T_c = T_c(0.9\rho_n) - T_c(0.1\rho_n)$, where $\rho_n$ is the resistivity of the sample above the transition[38], in the case of YPrBaCuO single crystal, is rather small. At P = 0, $\Delta T_c \approx 1.4$ K and $\Delta T_c \approx 2$ K at P = 1.7 GPa, which gives $d\Delta T_c/dP \approx 0.35\ K{\cdot}GPa^{-1}$. At the same time, in OD YBCO with $T_c = 91.07$ K, which does not contain defects, the resistive transitions are noticeably narrower, namely, $\Delta T_c \approx 0.3$ K (P = 0), $\Delta T_c \approx 0.5$ K (P = 0.95 GPa) and $d\Delta T_c/dP \approx 0.18\ K{\cdot}GPa^{-1}$ [39]. It is significant that in all the cases the pressure increases the resistive transition width. This effect is most pronounced in slightly doped (SD) YBCO single crystals ($T_c(P = 0) = 49.2$ K), where $d\Delta T_c/dP \approx 0.65\ K{\cdot}GPa^{-1}$ [38] and especially in HoBCO single crystals ($T_c(P = 0) = 61.3$ K, and $\mu_{Ho} \approx 10.5\mu_B$ and $m_{eff} = 9.7\mu_B$[12]), containing prolonged defects in the form of TB[46]. In the latter case, $d\Delta T_c/dP \approx 3.5\ K{\cdot}GPa^{-1}$. Resistive parameters of the samples under study at various pressures are given in Table 1.

Just as in the overwhelming majority of cuprates, in the YPrBaCuO single crystal under study, the hydrostatic pressure leads to the increase of $T_c$ at a rate $dT_c/dP = +1.82\ K{\cdot}GPa^{-1}$ and decreases the resistance as $d\ln\rho/dP = -(10.5 \pm 0.2)\ \%{\cdot}GPa^{-1}$ (Fig. 1, inset b, and Fig. 2a). However, there are some noticeable differences. Typically, in cuprates in the pressure range under consideration, the dependences of $T_c$, T*, and ρ on P are linear[27,31,47]. It is true not only for YBCO[25,46,48]. In our case, the dependence of $T_c$ on P is appreciably nonlinear and already comes to saturation at P ≥ 0.9 GPa (Fig. 1, inset b, and Fig. 2a). At this pressure the dependence ρ(300) on P also deviates from linearity towards higher values (Fig. 1, inset b). However, the most interesting pressure dependences are demonstrated by ρ (100), measured in the pseudogap region. So does the T*(P) (Fig. 2a,b). Both dependences clearly change the slope at P ~ 0.9 GPa. As it will be shown below, most of the measured parameters of YPrBaCuO demonstrate some peculiarity at P ~ 0.9 GPa.

We also note a very small, compared to pure YBCO single crystals with a similar $T_c = 85.2$ K[44], value of the PG temperature T* = 110 ± 0.3 K at P = 0. Any dopants, including Pr, may play the role of impurities in the sample, since their random Coulomb fields create additional scattering centres for charge carriers[16–18]. It can be assumed that additional defects induced by PrBCO, as well as the magnetic moment of PrBCO, prevent the establishment of phase coherence and the formation of fluctuating Cooper pairs (FCPs) above $T_c$, consequently reducing T*[18,24]. Another difference is in the relatively weak decrease of resistance under pressure, especially if one considers that the pressure in this case is 1.7 times greater than the pressure we employed in previous studies[38,39,46]. The obtained value $d\ln\rho/dP = -(10.5 \pm 0.2)\ \%{\cdot}GPa^{-1}$ is 1.6, and it 1.8 times less than in OD[39] and SD[38] pure YBCO single crystals, respectively. One of the possible reasons for the decrease in resistance is the redistribution of charge carriers under pressure from the CuO chains into the $CuO_2$ planes, which should lead to an increase in the density of charge carriers, $n_f$, in the planes[12]. As noted above, in YPrBCO part of the charge carriers is localized, which can suppress the rise of $n_f$ under pressure in the $CuO_2$ planes and lead to the observed decrease in the rate of ρ reduction. The observed unexpected increase in the PG temperature to T* = 122.9 ± 0.3 K at P = 1.7 GPa is discussed below.

In accordance with the phase diagram of cuprates[7–9,41], an increase in $n_f$ in the $CuO_2$ planes under pressure should lead to an increase in the $T_c$ of the samples (see review[12] and references therein). In the single crystal YPrBaCuO under study we have $dT_c/dP = +1.82\ K{\cdot}GPa^{-1}$ (Fig. 1, inset b). This is ~2.7 times less than in SD YBCO single crystals, where $dT_c/dP = +5\ K\ GPa^{-1}$ [38], but ~2.5 times higher than in OD of YBCO single crystals, where the increment rate of the critical temperature $dT_c/dP = +0.73\ K{\cdot}GPa^{-1}$ [39]. The $dT_c/dP$ observed in YPrBCO is approximately the same magnitude as it should be in pure YBCO with $T_c \approx 85$ K. Thus, the localization of charge carriers due to the presence of PrBCO in this case has little effect on $T_c$. This result once again confirms that the mechanisms of the effect of hydrostatic pressure on the critical temperature and the resistivity of both YPrBCO and YBCO single crystals, are most likely different[12,46].

While determining $dT_c/dP$, two effects should be distinguished, the first one associated with change in electron-phonon interaction, lattice parameters, bonding in-between layers, etc. (true pressure effect), and the second effect of change in $n_f$ due to redistribution of labile oxygen (pressure relaxation effect)[12,25–31]. The dependence of $T_c$ on pressure can be represented by the formula[25,49].

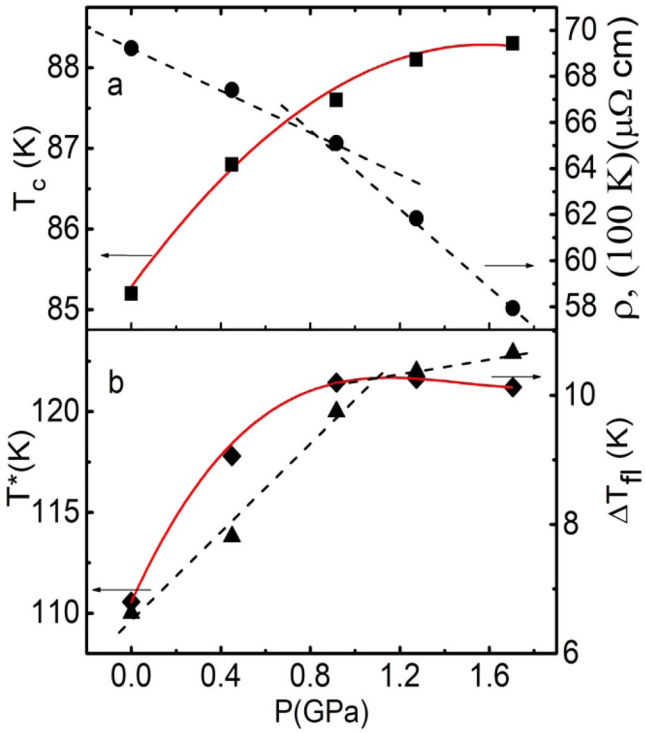


**Figure 2.** The pressure dependencies: $T_c$ (panel a, squares), T* (panel b, triangles), ρ(100 K) (panel a, dots) and $\Delta T_{fl}$ (panel b, diamonds) for $Y_{0.95}Pr_{0.05}Ba_2Cu_3O_{7-\delta}$ single crystal. The red curves are the 4th degree polynomial approximations. The dashed lines present the linear interpolation.

$$\frac{dT_c}{dP} = \left(\frac{\partial T_c}{\partial P}\right)_n + \left(\frac{\partial T_c}{\partial n}\right)_P \cdot \frac{dn}{dP} \tag{1}$$

where $n = n_f$ is the density of charge carriers in the sample. Thus, the first term on the right of Eq. (1) characterizes the true direct effect of pressure, and the second is the result of the change in $n_f$ under pressure. As was shown above, in YPrBCO, the change in $n_f$ is relatively small due to the possible localization of charge carriers. Therefore, it is the true pressure effect that should be responsible for $dT_c/dP$ in YPrBCO. Various theoretical models for describing the behaviour of $dT_c/dP$ in cuprates are discussed in detail previously[12]. The small $dT_c/dP$ values in the OD samples[39,47] and the noticeable effect of pressure on the $T_c$ value in the SD YBCO single crystals[38,47], observed in the experiment, can be explained in the framework of the model assuming the presence of a Van Hove singularity in the spectrum of charge carriers[50,51], which is characteristic to lattices with strong bonding. In OD crystals (with $T_c \sim 90$ K) the Fermi level is in the valley formed between the two peaks of the density of states. Importantly, the density of states at the Fermi level N ($E_F$) depends upon the orthorhombic distortion (a–b)/a[50]. It should be stressed that under hydrostatic pressure, the variation of the (a–b)/a ratio is small (it is determined only by the difference in compression modules along the a and b axes). Therefore, the change in $T_c$ under hydrostatic pressure is relatively small.

For SD crystals with low $T_c \sim 60$ K, the Fermi level can be shifted from the middle of the zone (among other factors due to doping with substitutional elements[52,53]) and is located away from the peak of the density of states. Therefore, if the critical temperature value is primarily determined by the density of electronic states, then a shift of the Fermi level towards the peak of the density of states, when the hydrostatic pressure is applied, can provoke a significant increase in the absolute value of $dT_c/dP$[25,38,47]. Accordingly, the crystals with intermediate values of $T_c$, including weakly Pr doped YPrBaCuO, should demonstrate intermediate values of $dT_c/dP$, as it is observed experimentally.

**Fluctuation conductivity.** Fluctuation conductivity (FLC) at all applied pressures was determined from the analysis of the excess conductivity σ′(T), which was calculated by the following equation as the difference between the measured resistivity ρ(T) and the linear normal-state resistivity of the sample $\rho_N(T) = aT + \rho_0$ extrapolated to low temperatures[39–42,54]:

$$\begin{aligned} \sigma'(T) &= \sigma(T) - \sigma_N(T) = [1/\rho(T)] - [1/\rho_N(T)], \text{ or} \\ \sigma'(T) &= [\rho_N(T) - \rho(T)]/[\rho(T)\rho_N(T)]. \end{aligned} \tag{2}$$

As shown in previous studies[42–44,55], the linear temperature dependence of the resistivity in the high temperature region is a distinctive feature of the normal state of cuprate HTSCs, for which stability of the Fermi surface

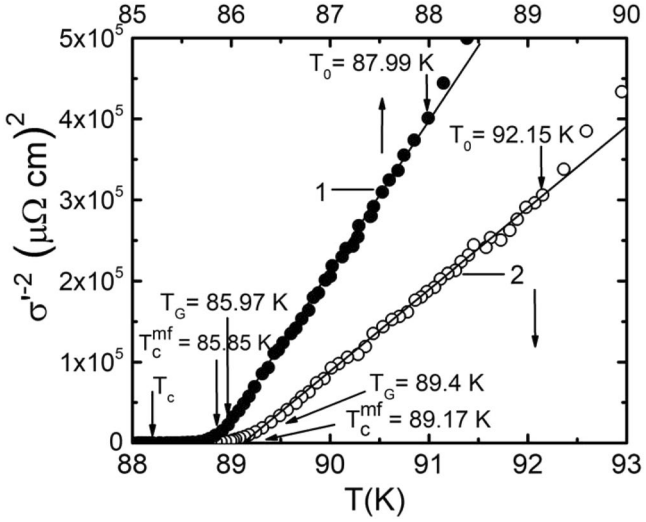


**Figure 3.** Temperature dependencies $\sigma'^{-2}(T)$ for $Y_{0.95}Pr_{0.05}Ba_2Cu_3O_{7-\delta}$ single crystal at P = 0 (curve 1, points) and P = 1.7 GPa (curve 2, circles) that define $T_c^{mf}$. The arrows point to the characteristic temperatures (refer to the text). The straight lines are to guide the eye.

takes place. Below the opening temperature of the pseudogap T* the Fermi surface may undergo rearrangement[7,9,55–57]. As a result, at $T \leq T^*$, not only practically all properties of HTSCs change and ρ(T) deviates from the linear dependence[57] but also the density of states at the Fermi level begins to decrease[58,59], which by definition is called a pseudogap[5–9,60]. Obviously, the resulting excess conductivity σ′(T), defined by Eq. (2), should contain information on the temperature dependence of both the FLC and PG[38,39,54,61]. This approach was used to analyze σ′(T) at all applied pressures. We consider below in more detail the procedure for determining the FLC and PG in the model of local pairs (LPs)[3–6,44,60] on the example of the samples Y0 (P = 0) and Y5 (P = 1.7 GPa).

Prior to beginning of the analysis within the framework of the LPs – model it is necessary to determine the critical temperature in the mean field approximation $T_c^{mf}$, which separates the FLC region from the region of critical fluctuations[12,60,62], i.e. the fluctuations of the SC order parameter Δ immediately near $T_c$ (where $\Delta < kT$), ignored in the Ginzburg-Landau theory[63]. The $T_c^{mf}$ is an important parameter of both FLC and PG – analysis, because it determines the reduced temperature

$$\varepsilon = (T/T_c^{mf} - 1) \tag{3}$$

which is present in all equations of this article. In HTSCs near $T_c$, the coherence length along the c axis, $\xi_c(T) = \xi_c(0)(T/T_c^{mf} - 1)^{-1/2}$ is greater than the corresponding unit cell size of YPrBCO d = c = 11.7 Å[64], and the FCPs interact in the entire volume of the superconductor. Accordingly, this is the area of 3D fluctuations. As a result, up to the temperature of the 3D – 2D crossover $T_0 > T_c^{mf}$, the σ′(ε) is always extrapolated by the fluctuation contribution of the Aslamazov – Larkin (AL) theory[65] for 3D systems[42,44,54,60].

$$\sigma'_{AL3D}(T) = C_{3D}\frac{e^2}{32\hbar\xi_c(0)}\varepsilon^{-\frac{1}{2}} \tag{4}$$

From this formula it is easy to obtain that $\sigma'^{-2}(T) \sim \varepsilon \sim T - T_c^{mf}$. Obviously, the extrapolated linear dependence $\sigma'^{-2}$ (T) turns to 0 just at $T = T_c^{mf}$ (Fig. 3)[62]. In addition to $T_c^{mf}$ and $T_c$, Fig. 3. also shows the Ginzburg temperature $T_G$, down to which the mean-field theories operate with decreasing T[27,63,66], and also the temperature of the 3D–2D crossover $T_0$, which limits the 3D – AL region of fluctuations from the top[27,44,60].

The significant difference between the results shown in Fig. 3, from the analogous dependences obtained on pure YBCO single crystals[12,38,39], is in the deviation of the experimental data leftwards and upwards from the linear dependence of $\sigma'^{-2}(T)$ above $T_0$. Such $\sigma'^{-2}(T)$ dependence indicates the absence of the fluctuation contribution of the Maki – Thompson (MT)[67] in the FLC and is typical for samples with defects[62,68]. In well-structured films[12,44,60] and single crystals of YBCO[38,39] the MT fluctuation contribution is always observed, and the experimental points above $T_0$ deviate to the right from the linear dependence $\sigma'^{-2}(T)$. The result confirms the above conclusion about the presence of additional defects in the sample induced by PrBCO[18,24,35,36]. The noticeable scatter of the experimental points in the temperature range $T_0 - T_G$ leads to a specific dependence of PG Δ*(T) in the specified temperature range, which will be discussed in what follows. Additionally, under pressure, the slope of the experimental curves noticeably changes (shown by the straight lines in Fig. 3). It is significant that the slope begins to change visibly only at P ≥ 0.9 GPa, indicating a non-monotonic increase in σ′(T) with increasing pressure. We emphasize that we did not find a change in the slope of the $\sigma'^{-2}(T)$ dependencies neither in the SD[38] nor in the OD[39] YBCO single crystals, however, it should be noted that the maximum value of P in these studies did not exceed 1 GPa.

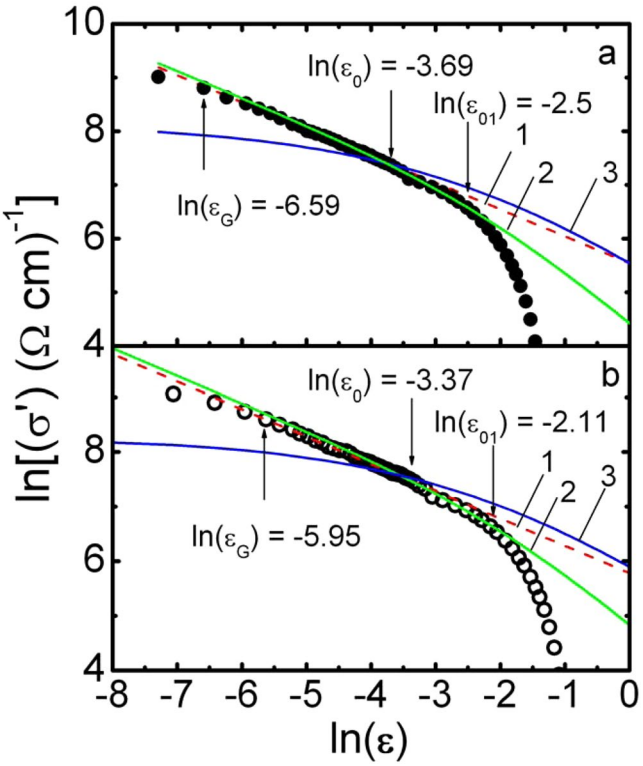


**Figure 4.** Dependence of $\ln\sigma'$ on $\ln\varepsilon$ of $Y_{0.95}Pr_{0.05}Ba_2Cu_3O_{7-\delta}$ single crystal for P = 0 (panel a, dots) and P = 1.7 GPa (panel b, circles) in comparison with fluctuation theories: AL – 3D (red dashed line 1), LD (green solid curve 2) and MT – 2D (blue solid curve 3).

Having determined $T_c^{mf}$, we find $\varepsilon$. After that we can clarify the role of fluctuating pairing in the formation of PG[3–8,60–62]. To do this, we construct the dependence $\ln\sigma'$ vs $\ln\varepsilon$, as shown in Fig. 4 for samples Y0 (P = 0) and Y5 (P = 1.7 GPa). As expected, regardless of the presence of pressure, near $T_c$ the FLC is perfectly approximated by the fluctuation contribution of AL for 3D systems (Eq. 4). In the logarithmic coordinates, the latter is plotted as dashed red straight lines (1) at Fig. 4 with slope $\lambda = -1/2$. This result confirms the above conclusion that classical 3D – AL FLC is always realized in cuprate HTSCs with $\xi_c(T) > d$ when T tends to $T_c$[12,27,41–44,69,70]. The linear dependence $\ln\sigma'$ ($\ln\varepsilon$) is maintained up to the temperature $T_0 = 88.0$ K ($\ln\varepsilon_0 = -3.69$, P = 0), at which the 3D-2D crossover occurs[67,71], and the experimental points deviate towards smaller values. At $T = T_0$, $\xi_c(T_0) = d = 11.67$ Å[44,60]. In accordance with previous studies[12,44,60] we obtain:

$$\xi_c(0) = d\sqrt{\varepsilon_0} \tag{5}$$

After getting $\varepsilon_0$ from the Eq. (5) we find $\xi_c(0) = (1.84 \pm 0.02)$ Å for P = 0. Similarly, the values of $\xi_c(0)$ are obtained at all other pressures (Table 1). These values of $\xi_c(0)$ are in reasonable agreement with the data reported for YBCO[27,38,39,72,73], and at P = 0 they actually coincide with $\xi_c(0) = (1.86 \pm 0.02)$ Å, found for the two-layer film YBCO-PrBCO with the similar $T_c = 85$ K (sample SD1)[23].

Above $T_0$ (Fig. 4) we have $\xi_c(T) < d$, and the sample loses its 3D state[42,44,67,71]. However, as before, in the temperature range $T_0 < T < T_{01}$ ($\ln\varepsilon_0 < \ln\varepsilon < \ln\varepsilon_{01}$, Fig. 4) $\xi_c(T) > d_{01}$ where $d_{01}$ is the distance between the inner conducting $CuO_2$ planes, and the $CuO_2$ planes are connected by the Josephson interaction[60,67,71]. As a result, two-dimensional (2D) FLC is realized in HTSC. However, in contrast to well-structured YBCO single crystals[30,38,39], in this case the temperature dependence of the FLC is described by the Lawrence – Doniach (LD) model (solid green curves 2 at Fig. 4)

$$\sigma'_{LD} = C_{LD}\frac{e^2}{16\hbar d\sqrt{1+2\alpha}}\varepsilon^{-1} \tag{6}$$

which is a special case of the Hikami – Larkin (HL) theory[67]. Here $\alpha = 2[\xi_c(0)/d]^2\varepsilon^{-1}$ is the coupling parameter. Near $T_c$, where $\xi_c(T) \gg d$, Eq. (6) is transformed into a 3D – AL (Eq. 4). Such temperature dependence $\sigma'(\varepsilon)$ is typical for HTSC samples with defects[62,68] arising under the influence of PrBCO. Accordingly, the fluctuation 2D-MT contribution to $\sigma'(\varepsilon)$ is

$$\sigma'_{MT2D} = C_{2D}\frac{e^2}{8d\hbar}\cdot\frac{1}{1-\alpha/\delta}\cdot\ln\left((\delta/\alpha)\cdot\frac{1+\alpha+\sqrt{1+2\alpha}}{1+\delta+\sqrt{1+2\delta}}\right)\cdot\varepsilon^{-1} \quad (7)$$

calculated for HTSCs in the HL theory[67]. It is characteristic to well-structured samples[12,38,39,44] and is completely suppressed in the given case. The MT contribution is determined by the pair-breaking processes in a sample in absence of the defects, i.e. it depends on the lifetime of the FCPs $\tau_\varphi$[67]:

$$\tau_\phi\beta T = \pi\hbar/8k_B\varepsilon = A/\varepsilon \quad (8)$$

where $A = 2.998\cdot10^{-12}$ sK and

$$\delta = \beta\frac{16}{\pi\hbar}\left(\frac{\xi_c(0)}{d}\right)^2 k_B T\tau_\phi \quad (9)$$

is the pair-breaking parameter. The factor $\beta = 1.203$ ($l/\xi_{ab}$) (where $l$ is the mean free path, $\xi_{ab}$ is the coherence length in the ab-plane) corresponds to the case of the clean limit ($l > \xi_{ab}$), which is always realized in HTSCs (see[12,60] and references therein). Curves (3), calculated using Eq. (7) with d = 11.67 Å and the values $\xi_c(0)$ determined from the experiment (Table 1), along with $\tau_\varphi$ (100 K) $\beta = 11.9\cdot10^{-13}$ s (P = 0), $\tau_\varphi$ (100 K) $\beta = 8.9\cdot10^{-13}$ s (P = 1.7 GPa), are also shown in Fig. 4 and, as expected, do not match the experiment.

Above $T_{01}$ [i.e. corresponding to $\ln\varepsilon_{01}$ at Fig. 4 ($T_{01} = 92.77$ K and $\ln\varepsilon_{01} = -2.5$, P = 0)], the experimental data deviate from the LD curve towards smaller values. Thus, classical fluctuation theories[65,67], based on the concept of the existence of incoherent FCPs in cuprate HTSCs at $T > T_c$[5,6,70], successfully describe the excess conductivity $\sigma'(T)$ only up to the temperature $T_{01}$. Above $T_{01}$ we have $\xi_c(T) < d_{01}$[12,23,60] and disappearance of the Josephson interaction between the inner conducting planes of $CuO_2$. In this case, both superconducting and normal charge carriers are confined directly in the $CuO_2$ planes, which are now not interconnected by any correlation interaction[67,71]. For this reason, above $T_{01}$ the fluctuation theories do not describe the experiment, as it is clearly seen from the results shown in Fig. 4. It is obvious that $\xi_c(T_{01}) = \xi_c(0)\varepsilon_{01}^{1/2} = d_{01}$. Since $\xi_c$ (0) is determined by the temperature of the 3D–2D crossover $T_0$ (Eq. 5), then the condition $\xi_c(0) = d\sqrt{\varepsilon_0} = d_{01}\sqrt{\varepsilon_{01}} = (1.84\pm0.02)$ Å (P = 0) must be fulfilled. Taking as noted above, d = c = 11.67 Å, for P = 0 we get $d_{01} = d\sqrt{\varepsilon/\varepsilon_{01}} = (6.43\pm0.05)$ Å and, respectively, $d_{01} = (6.22\pm0.05)$ Å for P = 1.7 GPa. Similarly, $d_{01}$ values were obtained for all other pressures (refer to Table 1). Thus, the pressure somewhat reduces the inter-plane distance in YPrBCO single crystals (refer to Fig. 4), which is reasonable[31,37] given that the pressure noticeably reduces all the parameters of the YBCO unit cell[74].

The fact that in the temperature range $\Delta T_{fl} = T_{01} - T_G$ FLC obeys the classical fluctuation theories means that $T_{01}$ is the temperature up to which the order-parameter phase stiffness, as well as the superfluid density $n_s$, have to maintain in HTSCs[5,6].

This is confirmed by the experiment[75–78]. Consequently, in this temperature range, the FCPs largely behave like the SC but non-coherent pairs (the so-called "short-range phase correlations"[4–6,23,41,70]), as noted above. Therefore, the problem of the temperature $T_{01}$ is very important. In some cases, e.g., $\Delta T_{fl} = 15.6$ K and $T_{01} \sim 16$ K is higher than $T_c$. This result, $T_{01}/T_c \approx 1.19$, was obtained on a well-structured two-layer YBCO-PrBCO film with $T_c = 88.5$ K (sample SD2)[23], in which independently deposited PrBCO layers do not create additional defects in the YBCO layers[19,23]. The similar film with $T_c = 85$ K (sample SD1 in[23]) is characterized by $\Delta T_{fl} = 11.4$ K and $T_{01}/T_c \approx 1.13$. In the YPrBCO single crystal under study with practically the same $T_c = 85.2$ K, the $\Delta T_{fl} = 6.8$ K and $T_{01}/T_c \approx 1.05$ at P = 0, i.e., it is 1.7 times less than in the well-structured SD1 film. This result once again confirms the conclusion that it is the defects induced by magnetic impurities in the form of PrBCO inclusions, arising in YBCO doped with Pr, which prevent the establishment of phase coherence of the FCPs and noticeably reduce the region of SC fluctuations. Under the pressure of 1.7 GPa, the critical temperature of the YPrBCO single crystal increases to $T_c = 89.1$ K becoming almost the same as in the SD2 film. Correspondingly, the range of SC fluctuations $\Delta T_{fl} = 10.13$ K as well as $T_{01}/T_c \approx 1.11$, i.e. increase noticeably (refer to Table 1). At the same time the C-factor $C_{3D}$ also increases, from 0.62 (P = 0) to 0.93 (P = 1.7 GPa), i.e., the better the sample structure, the closer $C_{3D}$ to unity[46,60]. Thus, it can be assumed that the pressure not only decreases $d_{01}$, but also reduces the number of defects in the sample, minimizing the degree of disorder, consistently with previous studies[28,74].

The increase in $\Delta T_{fl}$ also occurs non-monotonously. Up to P = 0.92 GPa, the range of SC fluctuations rapidly widens, and then comes to saturation (Fig. 2b, red curve). From Fig. 2. it can be seen that the dependence $\Delta T_{fl}$ (P) is essentially the same as the dependence $T_c$ (P). Taking into account the observed decrease in ρ(P) (Fig. 2a) it can be assumed that the reason for the increase in both $T_c$ and $\Delta T_{fl}$ is in growth of the density of charge carriers in the sample under applied P. For the first time such non-monotonic behaviour of all the functions (Fig. 2) was found. It can be attributed to specific features of the $Y_{0.95}Pr_{0.05}Ba_2Cu_3O_{7-\delta}$ single crystal under study.

**Temperature dependence of the pseudogap.** In the model of local pairs (LPs)[3–6,54,60,75–78], it is assumed that the deviation of ρ(T) from the linear dependence is due to opening of the PG at $T^* \gg T_c$, leading to appearance of the excess conductivity σ′(T), Eq. (1), as a result of formation of the LPs. This in turn means that the excess conductivity σ′(T) arising from such processes should contain information about the magnitude and temperature dependence of PG.

To obtain such information, one needs to have an equation that describes the experimental dependence of σ′(T) over the entire temperature range from T* to $T_c$ including the pseudogap parameter Δ*(T) in an explicit form. In view of the absence of a rigorous theory, the corresponding formula for σ′(T) was previously proposed[61]

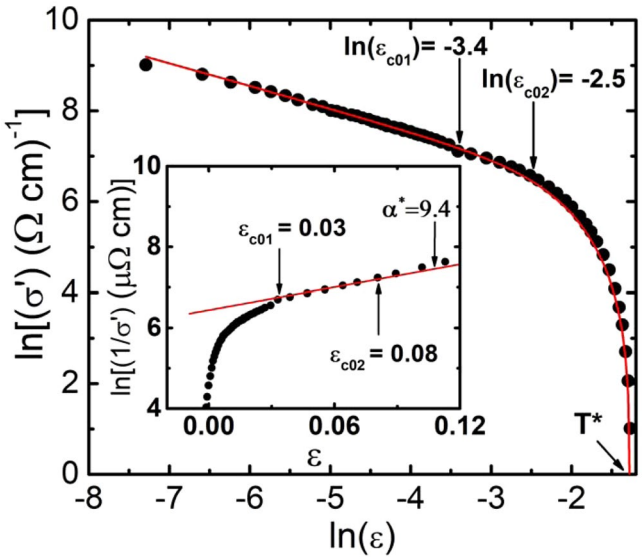


**Figure 5.** Dependence of $\ln(\sigma')$ vs $\ln(\varepsilon)$ (points) of the $Y_{0.95}Pr_{0.05}Ba_2Cu_3O_{7-\delta}$ single crystal for P = 0, plotted over the entire temperature range from T* to $T_c^{mf}$. The red curve is the approximation of the experimental data by Eq. (10). Inset: $\ln(\sigma'^{-1})$ as a function of ε. The red line marks the linear part of the curve, the inverse slope of which is $1/\alpha^* = \varepsilon_{c0}^* = 0.11$.

| P (GPa) | T* (K) | α | $\varepsilon_{c0}^*$ | $T_{pair}$ (K) | D* | Gi | $\Delta^*(T_G)$ (K) |
|---|---|---|---|---|---|---|---|
| **0** | 110 | 9.4 | 0.11 | 108 | 5 | 0.0014 | 216.13 |
| **0.45** | 113.8 | 6.5 | 0.15 | 109.7 | 5 | 0.0013 | 218.16 |
| **0.92** | 120 | 6.2 | 0.16 | 110.6 | 5 | 0.0015 | 220.83 |
| **1.27** | 122 | 5.5 | 0.18 | 114.6 | 6.0 | 0.0017 | 268.04 |
| **1.70** | 122.9 | 5.9 | 0.17 | 115 | 6.4 | 0.0026 | 290.02 |

**Table 2.** Transformation of the parameters used in the analysis of the PG behaviour in $Y_{0.95}Pr_{0.05}Ba_2Cu_3O_{7-\delta}$ single crystal under pressure.

$$\sigma'(\varepsilon) = \frac{e^2 A_4\left(1 - \frac{T}{T^*}\right)\left(\exp\left(-\frac{\Delta^*}{T}\right)\right)}{16\hbar\xi_c(0)\sqrt{2\varepsilon_{c0}^*\sinh(2\varepsilon/\varepsilon_{c0}^*)}} \tag{10}$$

where $(1 - T/T^*)$ determines the number of pairs appearing at $T \leq T^*$, and $\exp(-\Delta^*/T)$ gives the number of pairs destroyed by thermal fluctuations below $T_{pair}$. Solving Eq. (10) for $\Delta^*(T)$, we obtain the equation for PG

$$\Delta^*(T) = T \ln \frac{e^2 A_4\left(1 - \frac{T}{T^*}\right)}{\sigma'(T)16\hbar\xi_c(0)\sqrt{2\varepsilon_{c0}^*\sinh(2\varepsilon/\varepsilon_{c0}^*)}}, \tag{11}$$

where $\sigma'(T)$ is the excess conductivity experimentally determined.

In addition to $T_c^{mf}$, T*, $\xi_c(0)$ and ε, that are already defined above, Eqs. 10 and 11 contain the coefficient $A_4$, which has the same meaning as the C-factor in the theory of FLC, and also Δ* along with the theoretical parameter $\varepsilon_{c0}^*$[72,73], which determines the shape of theoretical curves for $T > T_{01}$[60,61]. Within the framework of the LPs model, all these parameters are also directly determined from experiment[23,24,38,39,61]. In order to find $\varepsilon_{c0}^*$, we use the experimental fact that in the interval $\ln\varepsilon_{01} < \ln\varepsilon < \ln\varepsilon_{02}$ ($\ln\varepsilon_{01} = -3.4$; $\ln\varepsilon_{02} = -2.5$, at Fig. 5) the excess conductivity $\sigma'^{-1} \sim \exp(\varepsilon)$, which is apparently an intrinsic property of cuprates[23,61,72,73]. Accordingly, in the temperature range $\varepsilon_{c01} < \varepsilon < \varepsilon_{c02}$ ($89.2 < T < 92.8$ K) (see inset to Fig. 5), $\ln(\sigma'^{-1})$ is a linear function of ε with the slope $\alpha^* = 9.4$, which defines the parameter $\varepsilon_{c0}^* = 1/\alpha^* = 0.11$ at P = 0[72,73]. The similar graphs with $\alpha^*$ decreasing to 5.9, which gives $\varepsilon_{c0}^* \approx 0.17$ at P = 1.7 GPa, were plotted for all other pressure values. The latter allowed us to obtain the reasonable values of $\varepsilon_{c0}^*$, which tend to increase with P, as can be seen from Table 2.

To find $A_4$, using Eq. 10, it is necessary to calculate the dependence $\sigma'(T)$ and, selecting $A_4$, combine with the experiment in the region of 3D – AL fluctuations (solid red curve at Fig. 5), where $\ln\sigma'$ is a linear function of $\ln\varepsilon$ with the slope $\lambda = -1/2$[42,44,60]. However, Δ* still remains undetermined. While using Eq. 10 we take into account the results of works[77,78] and assume Δ* equal to $\Delta^*(T_G) = \Delta(0)$, where Δ(0) is the SC gap at T = 0, as noted above. Accordingly, the following relation should be satisfied: $D^* = 2\Delta^*(T_G)/k_BT_c = 2\Delta(0)/k_BT_c$[12,23,60]. Ultimately, to estimate $\Delta^*(T_G)$, which is used in Eq. 10 we plot $\ln\sigma'$ as a function of $1/T$[23,54,61]. The results for P = 0 and P = 1.7 GPa

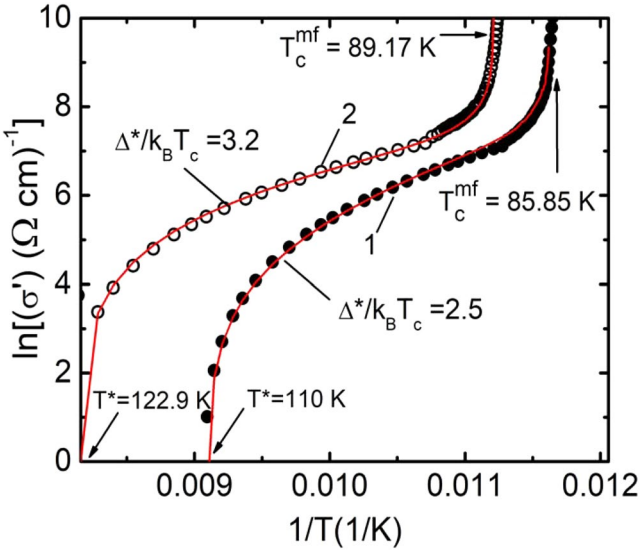


**Figure 6.** $\ln\sigma'$ as a function of 1/T for a $Y_{0.95}Pr_{0.05}Ba_2Cu_3O_{7-\delta}$ single crystal over the entire temperature range from $T^*$ to $T_c^{mf}$ at P = 0 (curve 1, points) and P = 1.7 GPa (curve 2, circles). Red curves - approximation of the data by Eq. 10 with $\Delta^*(T_G) = 2.5$ K (P = 0) and $\Delta^*(T_G) = 3.2$ K (P = 1.7 GPa).

are shown at Fig. 6. In this case, the shape of the theoretical curve turns out to be very sensitive to the value of $\Delta^*(T_G)$. The best approximation for P = 0 is achieved at $\Delta^*(T_G) = 2.5\ k_BT_c$, i.e. $D^* = 5.0 \pm 0.1$ (curve 1 at Fig. 6), which is the typical value for the d-wave superconductors in the strong coupling limit at ambient pressure[12,61,79,80].

This result seems reasonable, given that the sample is OD in oxygen, with a high $T_c = 85.2$ K even in the presence of Pr. For P = 1.7 GPa, respectively, we obtain $\Delta^*(T_G) = 3.2\ k_BT_c$ or $D^* = 6.4 \pm 0.1$ (curve 2 in Fig. 6). It can be seen that for the chosen values of the parameters the calculated curves perfectly describe the experiment, including the data at Fig. 5, thus confirming the validity of the present approach. Similar graphs were obtained for all the pressure values chosen, which made it possible to obtain reliable $\Delta^*(T_G)$ and D* values for all the samples (refer to Table 2). It is also seen from the figure that the pressure significantly increases the value of the excess conductivity $\sigma'$, especially in the high-temperature region. However, it is necessary to point out the threshold nature of the results obtained. Namely, the change in the value of the parameter D* derived from the experimental curves begins only above P ~ 0.9 GPa (see Table 2).

Since all the necessary parameters have been found, we can construct the dependences $\Delta^*(T)$ for all pressure values. The fact that Eq. 10 perfectly approximates the experimental data (Figs. 5 and 6) allows us to conclude that calculated by Eq. 11 dependences $\Delta^*(T)$ will gain the correct values and temperature dependencies of PG. The function $\Delta^*(T)$ for P = 0 based on the experimentally determined parameters $T^* = 110$ K, $T_c^{mf} = 85.85$ K, $\xi_c(0) = 1.84$ Å, $\varepsilon_{c0}^* = 0.11$ and $A_4 = 34$ is shown at Fig. 7 as solid dots. Accordingly, $\Delta^*(T)$ for P = 1.7 GPa is plotted at Fig. 7 in empty circles. This curve was based on the parameters $T^* = 122.9$ K, $T_c^{mf} = 89.17$ K, $\xi_c(0) = 2.16$ Å, $\varepsilon_{c0}^* = 0.17$, $A_4 = 85$. Similar dependences $\Delta^*(T)$ for P = 0.45, 0.92 and 1.27 GPa based on the parameter sets given in Tables 1 and 2 are located between these two curves but are not shown here for the sake of not complicating the figure. The pressure noticeably increases the $\Delta^*(T)$ (Fig. 7). Using the data of Table 2 we find that under the pressure $\Delta^*$ and D* increase as $d\ln\Delta^*/dP = 0.17\ GPa^{-1}$. We emphasize that for making $d\ln\Delta^*/dP$ estimates we took the values of $\Delta^*(T_G)$, which, as noted above, can be considered as an analogue of the SC gap $\Delta(0)$[12,77,78]. Thus, the hydrostatic pressure increases both $\Delta^*$ and respectively D*, which is consistent with the results of[31,38,39,81], where an increase under pressure in both PG and SC gap $\Delta$, as well as increase of the BCS relationship $2\Delta(0)/k_BT_c$, is reported.

However, the values of the derivatives $d\ln\Delta^*/dP = 0.17\ GPa^{-1}$ for the samples with Pr doping are almost two times less than $d\ln\Delta^*/dP = 0.32\ GPa^{-1}$ and $d\ln\Delta^*/dP = 0.36\ GPa^{-1}$ measured for the OD and SD YBCO single crystals[38,39], respectively. In accordance with previous studies[12,38,39,46,60,81], the experimentally observed increase in $T_c$ under pressure should lead to an increase in both the SC gap $\Delta$ and the PG $\Delta^*$. Interestingly, in pure OD single crystals of YBCO the $T_c$ increases only by 0.7 K, while $d\ln\Delta^*/dP = 0.32\ GPa^{-1}$. In the YPrBCO single crystal under study $T_c$ increases by 3 K, and $d\ln\Delta^*/dP = 0.17\ GPa^{-1}$. Thereby there is no direct correlation between the growth of $T_c$ and the value $d\ln\Delta^*/dP$ in this case. As already mentioned, under the hydrostatic pressure the increase in $T_c$ may occur due to rising of the density of charge carriers $n_f$ in the $CuO_2$ planes[12,25–31] and due to the convergence of the peaks of the density of states[52,53]. Taking into account the results obtained, it is possible to conclude that in YPrBCO the influence of the both given processes on $d\ln\Delta^*/dP$ is relatively weak due to possible partial localization of the charge carriers[18,19,36], presence of defects and intrinsic magnetism of PrBCO[21–23]. Another possible mechanism responsible for the increase in the SC gap and the PG is associated with a shift towards lower frequencies of the phonon spectrum of a superconductor under pressure[81]. However, how this mechanism works in presence of the magnetic PrBCO is not clear, and this question remains open.

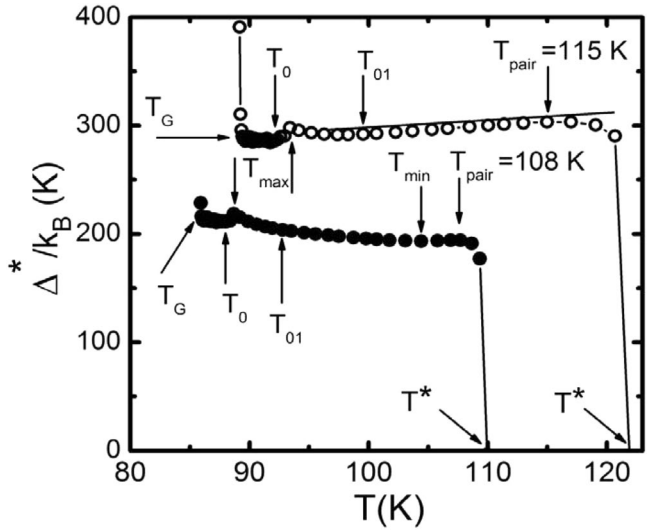


**Figure 7.** Temperature dependences of the pseudogap $\Delta^*(T)$ of $Y_{0.95}Pr_{0.05}Ba_2Cu_3O_{7-\delta}$ single crystal, calculated from Eq. (11), at P = 0 (points) P = 1.7 GPa (circles). The arrows indicate the characteristic temperatures $T_{pair}$, $T_{min}$, $T_{max}$, $T_{01}$, $T_0$ and $T_G$. The solid line is to guide the eye.

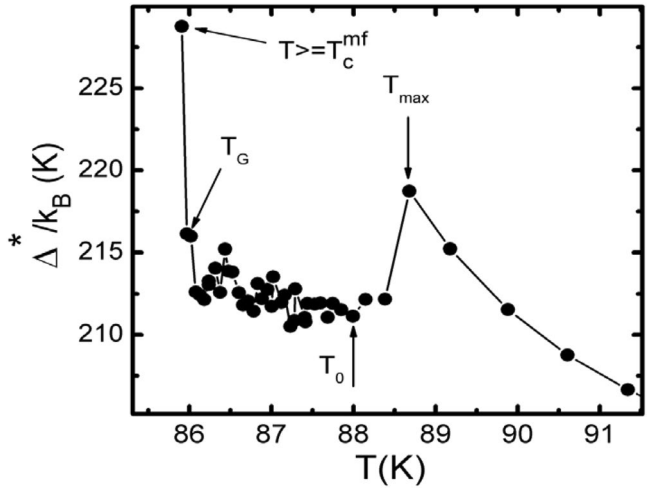


**Figure 8.** The dependence $\Delta^*(T)$ in $Y_{0.95}Pr_{0.05}Ba_2Cu_3O_{7-\delta}$ single crystal near $T_c$ calculated by Eq. (11) with the parameters given in the text for P = 0 (points). The arrows indicate the characteristic temperatures $T_{max}$, $T_0$, $T_G$ and $T_c^{mf}$. The solid curve is to guide the eye.

It is seen from Fig. 7. that at P = 0 GPa the shape of the $\Delta^*(T)$ curve is quite unusual, namely at $T < T_{pair} = 108$ K a weakly pronounced minimum is observed that corresponds to $T_{min} \approx 103$ K. Below $T_{min}$ the $\Delta^*(T)$ grows uniformly showing a maximum at $T_{max} = 88.7$ K, where $\Delta^*(T_{max}) = 218.7$ K. It is significant that this maximum is ~ 0.7 K above $T_0 = 88.0$ K, which was determined from the FLC analysis (Fig. 3). With further reduction of T the $\Delta^*(T)$ abruptly decreases by ~6.5 K, and $\Delta^*(T_0) = 212.2$ K. Most likely, the observed maximum and the jump in $\Delta^*(T)$ are due to the inertia of the measuring system that reflects a reaction to change in the cooling rate in the interval 93 K–88 K coinciding with the change in measurement step from $\delta T = 1$ K at $T > 93$ K to $\delta T = 0.1$ K at $T < 88$ K (Fig. 1). Below $T_0$ there is a large scatter of experimental points, which ends with a maximum of $\Delta^*(T_G) = 216.1$ K at $T = T_G$, as shown in detail at Fig. 8. The same type voltage jumps near $T_c$ were observed when studying the Hall effect on the $Y_{0.9}Pr_{0.1}Ba_2Cu_3O_{7-\delta}$ film (see Fig. 3 in[82]), which is a manifestation of specific behaviour of HTSCs containing PrBCO magnetic impurities directly inside the YBCO matrix[18,36,82]. It can also be seen that it is precisely below $T_G$ the transition to the area of the critical fluctuations begins. However it is possible to obtain yet another point, which is 0.05 K above $T_c^{mf}$. The similar behaviour of $\Delta^*(T)$ below $T_{max}$ is also demonstrated by the single crystal under study at P = 1.7 GPa (circles at Fig. 7).

The dependences $\Delta^*(T)$ obtained significantly differ from the analogous $\Delta^*(T)$, which we observed in the region of SC fluctuations near $T_c$ in all cuprates and pnictides studied previously[12,18,38,39,60]. For all of the mentioned HTSCs the $\Delta^*(T)$ always shows a minimum with decrease of temperature at $T \sim T_{01}$ and then a maximum

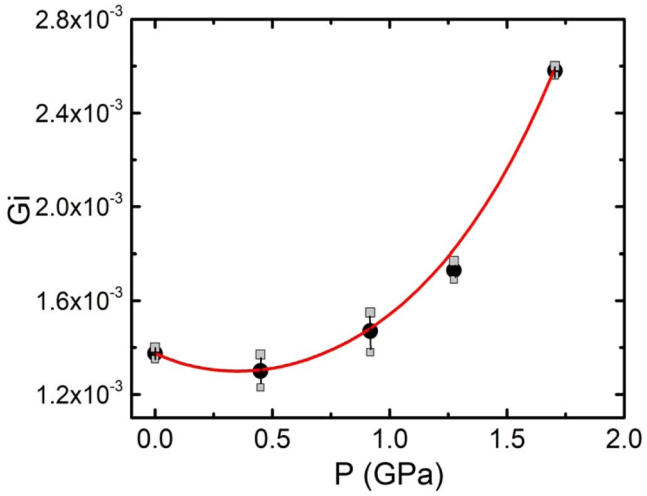


**Figure 9.** Ginzburg number $Gi = (T_G - T_c^{mf})/T_c^{mf}$ as a function of pressure for the $Y_{0.95}Pr_{0.05}Ba_2Cu_3O_{7-\delta}$ single crystal. The red curve is an extrapolation of the experimental data by a polynomial.

at $T \sim T_0$ followed by a minimum always at $T = T_G$. We underline that the same type dependence $\Delta^*(T)$ is also observed on superlattices and two-layer films of YBCO-PrBCO[23] in which, as already mentioned, independently deposited PrBCO films do not distort the structure of YBCO layers[19]. Thus, the correlation between the temperatures $T_{01}$, $T_0$, $T_G$ and the features (minima and maxima) in the $\Delta^*(T)$ dependence observed in the HTSCs listed above is clearly absent in the $Y_{0.95}Pr_{0.05}Ba_2Cu_3O_{7-\delta}$ single crystal under study.

From Fig. 7 it is also seen that the pressure not only increases $\Delta^*(T)$, but also changes the shape of the $\Delta^*(T)$ curve, that we have never observed on pure OD YBCO single crystals[12,39]. With increasing the pressure, the maximum at $T_{pair}$ becomes wider and is shifted to higher temperatures. Finally, at $P = 1.7$ GPa the dependence $\Delta^*(T)$ takes the form close to that observed for OD YBCO single crystals, demonstrating a falling linear dependence $\Delta^*(T)$ in the interval $T_{pair} > T > T_{01}$[39]. The latter indicates a strong influence of pressure on the dynamics of the lattice[28,31,37,74], especially in the high temperature range. Recall that $T_{pair}$ is the temperature at which local pairs are transformed from strongly bound bosons obeying the Bose-Einstein condensation theory (BEC) into the FCPs, which obey the Bardeen-Cooper-Schrieffer theory (BCS) (refer to[5,6,8,61,83] and references therein). In other words, this is the BEC-BCS crossover temperature predicted by the theory[84,85] for systems with the low density of charge carriers which are cuprate HTSCs with doping less than optimal[13,60,83]. As the temperature decreases below $T_{01}$ the $\Delta^*(T)$ increases showing a maximum at $T = T_{max} \approx 93.4$ K, where $\Delta^*(T_{max}) = 298.2$ K (circles at Fig. 7). This is where the similarity with the $\Delta^*(T)$ curve obtained for OD YBCO ends, since the non-standard behaviour of $\Delta^*(T)$ begins below $T_{max}$, which resembles the Pr effect on $\Delta^*(T)$ at $P = 0$. In the interval $T_{max} - T_0$, there is also a jump of $\Delta^*(T)$, the nature of which is most likely the same as in the case of $P = 0$. Then, similarly to $P = 0$, at $P = 1.7$ GPa there is a region characterized by large scatter of $\Delta^*(T)$ values ending with a maximum of $\Delta^*(T_G) = 290.0$ K at $T_G = 89.4$ K.

Notably, in this case it is possible to confidently measure the values of $\Delta^*(T)$ for three more temperatures below $T_G$ (Fig. 7, circles). Moreover, the last point was obtained at the temperature of 89.18 K which is only 0.01 K above the $T_c^{mf}$. This is most likely to occur because the pressure, broadening the SC transition, also increases the area of critical fluctuations[24,49]. Accordingly, the Ginzburg number, $Gi = (T_G - T_c^{mf})/T_c^{mf}$, also increases[27,46] (refer to Fig. 9). Thus, the difference $T_G - T_c^{mf}$ in fact increases (Table 1) indicating that the genuine critical fluctuations increase with pressure[27,46]. In accordance with the anisotropic Ginzburg – Landau theory, the Ginzburg number is determined by[66,86]:

$$Gi = \alpha \left( \frac{k_B}{\Delta c \xi_c(0) \xi_{ab}^2(0)} \right)^2 \tag{12}$$

where $\alpha$ is a constant of the order of $10^{-3}$ and $\Delta c$ is the jump in the heat capacity at $T_c$. In accordance with the microscopic theory[86], $\Delta c \sim T_c N(0)$, where $N(0)$ is the density of single-particle states at the Fermi level. It is assumed that $\Delta c$ weakly depends on P in the pressure range under consideration, since $N(0)$, as follows from measurements of the Pauli susceptibility above $T_c$, reacts weakly to a change in P (see[27,66] and references therein).

At any rate we are interested in the value of the ratio $Gi^* = Gi(P)/Gi(0)$[46], which depends only on the ratio of the coherence lengths. Using the data from Tables 1 and 2 we get: $Gi^* \approx 1.86$ and $\xi_c(P)/\xi_c(P = 0) \approx 1.17$. Thus, $\xi_c(0)$ increases with pressure by about 17% as $d\xi_c(0)/dP \approx 0.19$. Interestingly, an increase in $\xi_c(0)$ under pressure was also observed on YBCO[27,39], HoBCO[46], and HgBaCaCuO[48]. Moreover, $d\xi_c(0)/dP$ changes in the range from 0.08[39,48] to 0.42[46].

At a first glance, this is an amazing result, since $T_c$ simultaneously increases, and in the general theory of superconductivity it is assumed that $\xi \sim 1/T_c$[63]. However an increase in $\xi_c(0)$ with increasing P leads to enhancing of the coupling strength between the $CuO_2$ planes, $J = [\xi_c(0)/d]^2$[49] namely, $J(P)/J(0) \approx 1.38$, that is, the coupling strength increases by 38%. If we assume that in this case $d = d_{01}$, which seems reasonable, then $J(P)/J(0) \approx 1.47$, that is, the coupling strength between the $CuO_2$ planes under pressure increases almost 1.5 times. The result obtained shows

that under the influence of pressure, the simple ratio $\xi_c \sim 1/T_c$ in cuprates is violated, and emphasizes the strong anisotropy of the conductive properties in HTSCs[13,57,60]. Considering the above results and using Eq. 12 we find $\xi_{ab}(0)/\xi_{ab}(P) \approx 1.26$. That is to ensure the resulting increase in Gi* the $\xi_{ab}(0)$ should decrease by ≈26%.

Thus, as in OD YBCO[27,39], in the YPrBCO single crystal under study, the pressure affects both the properties of the sample along the c-axis and the $CuO_2$ conducting planes. This is in reasonable agreement with published data[27,46,66,87], as well as with the conclusions of the general theory of superconductivity, according to which the coherence length that determines the size of the Cooper pairs (in this case it is $\xi_{ab}$ (T)) is proportional to $1/T_c$[63]. Now, if our reasoning is correct, we can estimate the value of $\xi_{ab}$ (P = 1.7 GPa). Taking for the HTSCs as usual $\xi_{ab}(0) \sim 10\ \xi_c(0) \approx 18.4$ Å (P = 0)[60], we obtain: $\xi_{ab}(0)$ (P = 1.7 GPa) = 18.4 - (18.4 × 0.26) ≈ 13.6 Å. Such a value of $\xi_{ab}(0)$ is typical for defect-free YBCO films with doping, slightly lower than the optimum one[44,60,62], which confirms the validity of our estimates. It remains to add that, just like the other parameters measured, the Gi(P) in YPrBCO demonstrates non-monotonic dependence on pressure. From Fig. 9. it can be seen that the character of the dependence Gi(P) changes dramatically, and again at P > 0.9 GPa. It should be noted that a similar dependence Gi(P) was observed previously[27]. The YBCO single crystals studied by Ferreira *et al.*[27] contained a large number of twin defects. Accordingly, the pressure could minimize the influence of defects, leading to a similar dependence Gi(P). However, this question was not considered by Ferreira *et al.*[27].

There are a number of differences we identified in the behaviour of YPrBaCuO in comparison with pure YBCO single crystals. First of all the unexpected increase in T* under pressure takes place (Fig. 7 and Table 2). In accordance with the phase diagram of cuprates[7,9,12,41], with increasing $T_c$ (in this case by application the pressure), T* should decrease, as is observed in defect-free OD and SD YBCO[38,39] and also in HoBCO[46] single crystals. In YPrBaCuO, an extremely low T* ~ 110 K at P = 0 (Fig. 1 and Table 2), characteristic of compounds containing Pr impurities[18], is initially observed. This result can be explained in the assumption that the defects produced by PrBCO and PrBCO's intrinsic magnetism effectively disturb the exchange interaction between electrons, preventing the formation of the FCPs[18,36,60] as noted above.

Accordingly, the observed effect of increasing T* becomes clear, if we assume that pressure, improving the structure[28,31,37,74], minimizes the effect of defects. This is confirmed by a decrease in sample resistance (Fig. 1), an increase in $\Delta T_{fl}$ and coefficient $C_{3D}$ (Table 1), as well as an appropriate transformation of the dependence Δ*(T) (Fig. 7). Thus, the present results indicate that, under a pressure of 1.7 GPa, the YPrBaCuO under study is likely to transform into a practically defect-free YBCO single crystal, and the PG temperature is restored to T* ~ 123 K (Fig. 2 and Table 2). However, at the same time $T_c$ increases by about 3 K (Table 1) which should lead to a decrease in T*, as we noted above. Thus, in this case, two opposite effects are most likely to occur: (a) an increase in T* under pressure due to minimization of the effect of additional defects, (b) a decrease in T* with an increase in $T_c$ of the sample.

We can assume that if there were no effect of Pr, the YBCO single crystal under study, at P = 0 would have T* ~ 140 K, which is a typical value for OD of YBCO[72,73,77,78]. In pure OD YBCO single crystals under P ≈ 0.95 GPa, an increase in $T_c$ by only 0.7 K leads to a decrease in T* by 5 K[39]. In our case, at P ≈ 0.95 GPa, $T_c$ increases by ~2.4 K (Table 1), that is, ~3.4 times more than in an OD single crystal not containing Pr. Accordingly, the reduction of T* should be: ΔT* ≈ 3.6 × 5 = 17 K. In other words, the pressure P = 1.7 GPa, reducing the influence of defects, restores T* to the observed value T* = 140 K–17 K = 123 K, confirming the assumption made. Here we also considered that both $T_c$ and T* reach saturation at P > 1 GPa (Figs. 1 and 2).

The dependence of the relation $D^* = 2\Delta^*(T_G)/k_BT_c$ on pressure was also unusual (Fig. 10, curve 1). In contrast to OD (curve 2) and SD (curve 3) of pure YBCO single crystals, up to P ~ 0.9 GPa the D* in YPrBCO does not change, conserving the values equal to ~5 (Fig. 10 and Table 2). At P > 0.9 GPa, a sharp increase in D* is observed, and, curiously, the dependence comes to a straight line, which is the continuation of the linear dependence D*(P) (dashed line in the figure) demonstrated by the OD single crystal. Thus, as noted above, it can be assumed that the pressure improves the structural order in the sample[28,37,40] and minimizes the effect of defects in YPrBaCuO, the number of which at the given Pr content is probably relatively small. As a result, at P > 1 GPa, the D*(P) dependence becomes the same as in a defect-free YBCO single crystal, where, unfortunately, the measurements were performed only up to P = 0.95 GPa[39]. Summarising the results, we can conclude that, at P > 1 GPa, the YPrBCO single crystal behaves to a large extent as an YBCO single crystal with a relatively small number of defects. As noted above, this is confirmed by the dependence Δ*(T), measured at P = 1.7 GPa, whose shape at high T is the same as in OD YBCO single crystals (Fig. 7, circles), and also by a noticeable increase in $\Delta T_{fl}$ and $C_{3D}$ with pressure (refer to Table 1). Attention is drawn to the fact that the growth of D* begins only after ~0.9 GPa.

In the same way increases Δ*, which measured at $T_G$ (Table 2). It is curious that the same type threshold effect is observed when the slope of the $\sigma'^{-2}(T)$ dependences is changed (Fig. 3), so is the Ginzburg number Gi under pressure (Fig. 9), and, in fact, all of the measured parameters exhibit some threshold dependence. We believe that all the features determined are due to the specific influence of additional defects, as well as the PrBCO intrinsic magnetism. Naturally, these nontrivial results require further investigation and we expect the present study to motivate the community.

## Conclusion

For the first time, the effect of hydrostatic pressure up to 1.7 GPa on the temperature dependence of the excess conductivity σ′(T) and the PG of the $Y_{1-x}Pr_xBa_2Cu_3O_{7-\delta}$ single crystal (x ≈ 0.05) was experimentally studied. It is shown that when the hydrostatic pressure is applied, the resistivity ρ(T) decreases with the rate $d\ln\rho(100K)/dP = -(10.5 \pm 0.2)\%\ GPa^{-1}$, while the critical temperature increases with the rate $dT_c/dP = +1.82\ K \cdot GPa^{-1}$ that is consistent with the literature data. It was determined that, regardless of the external pressure, the excess conductivity σ′(T) in the interval $T_c < T < T_{01}$ is described by the classical fluctuation theories, namely the 3D Aslamazov-Larkin theory (Eq. 4) and Lawrence-Doniach (LD) theory (Eq. 6). The fluctuation contribution of the Maki-Thompson (Eq. 7) is not observed, which indicates the presence of defects in the sample induced by PrBCO cells embedded in the YBCO matrix. Moreover, the dopant has intrinsic magnetic moment μPrBCO ≈2μB.

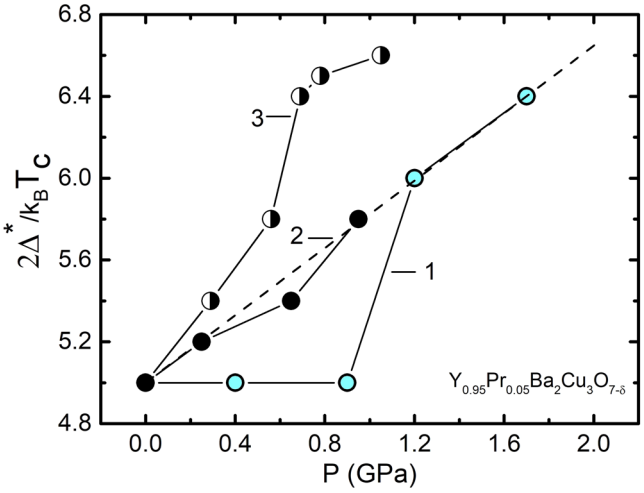


**Figure 10.** Dependences $D^* = 2\Delta^*(T_G)/k_BT_c$ on pressure for $Y_{0.95}Pr_{0.05}Ba_2Cu_3O_{7-\delta}$ single crystals (curve 1, circles), OD $YBa_2Cu_3O_{7-\delta}$ (curve 2, points) and SD $YBa_2Cu_3O_{7-\delta}$ (curve 3, half-empty circles). All the lines are to guide the eye.

The presence of defects led to the observation of a number of unusual effects. Among them is a small value of the region of SC fluctuations, $\Delta T_{fl} = 6.8$ K, and a very small (for the cuprates with $T_c = 85.2$ K) value of $T^* = 110$ K. It is assumed that the defects produced by PrBCO as well as its intrinsic magnetism effectively disturb the exchange interaction between electrons, preventing the formation of the FCPs. Under pressure, T* increases to ~ 123 K. Such behaviour of T* is unusual as according to the phase diagram of cuprates, the T* should decrease with increasing $T_c$. The observed effect of increasing T* becomes clear, if we assume that pressure, improving the structure, minimizes the effect of defects and restores the value of T*. This is confirmed by a decrease in sample resistance (Fig. 1), a noticeable increase in $\Delta T_{fl}$ and a $C_{3D}$ coefficient (Table 1), as well as a corresponding transformation of the dependence $\Delta^*(T)$ (Fig. 7). Simultaneously, the pressure reduces the distance between the conducting layers $d_{01}$, but increases $\xi_c(0)$ (Table 1). A decrease in $d_{01}$ seems reasonable, since the pressure reduces all the dimensions of the unit cell. The increase in $\xi_c(0)$ is also observed in a number of other works, and is explained when analyzing the Ginzburg parameter [(Eq. (12)].

It is shown that the shape of the dependence of the PG parameter, $\Delta^*(T)$, calculated according to Eq. (11), at $P = 0$ is rather unusual, with a weakly pronounced minimum at 103 K = Tmin <Tpair = 108 K (Fig. 7). The pressure noticeably changes the shape of the $\Delta^*(T)$ curve, which is not observed on pure OD YBCO single crystals. At $P = 1.7$ GPa, the shape of $\Delta^*(T)$ becomes the same as in OD of YBCO, confirming the assumption about minimization of the effect of defects under pressure. At the same time, there is an increase in $\Delta^*(T)$ and D* (Fig. 7) as $d\ln\Delta^*/dP = 0.17$ GPa$^{-1}$, which, however, is almost two times less than $d\ln\Delta^*/dP = 0.32$ GPa$^{-1}$ measured for OD YBCO single crystal. As is known, the change in the parameters of cuprates under the action of hydrostatic pressure, and above all, the growth of Tc can occur both due to an increase in the density of charge carriers nf in the $CuO_2$ planes, and due to the convergence of peaks of the density of states. Considering the present results, it can be concluded that in YPrBCO, the influence of both these processes is relatively small due to the likely localization of part of the charge carriers, the presence of defects and the intrinsic magnetism of PrBCO.

We note more nontrivial results that are not observed on the pure YBCO single crystals. These are the nonlinear character of the dependences of Tc and ΔTfl on P and a sharp change in the character of the pressure dependences ρ(100 K) and T* at T ≥ 0.9 GPa (Fig. 2). Moreover, the change of virtually all measured parameters with pressure has a threshold character. Thus, the slope of the dependences σ′-2(T) (Fig. 3), the growth of σ′(T), the shape of the curves ln(σ′) vs (1/T) (Fig. 6) and the Ginzburg parameter (Fig. 9) begin change only at P ≥ 0.9 GPa. This effect is most clearly observed in the D*(P) dependence (Fig. 10), which is determined with the highest accuracy. Unlike the OD and SD pure YBCO single crystals (curves 2 and 3 in Fig. 10), D* in YPrBCO does not change up to P ~ 0.9 GPa, keeping the value equal to ~5 (Table 2). At P > 0.9 GPa, a sharp increase in D* is observed, and the points fall on a straight line, which is a continuation of the D*(P) dependence in the defect-free OD YBCO single crystal. This result confirms the assumption that pressure improves the structural order in the sample and, thus, minimizes the effect of defects in Y0.95Pr0.05Ba2Cu3O7-δ. To conclude all the features found are due to the specific influence of additional defects produced by Pr, as well as by the intrinsic magnetism of PrBCO. These non-trivial results require further study.

## Experimental Methodology

$Y_{1-x}Pr_xBa_2Cu_3O_{7-\delta}$ single crystals were grown by the solution-melt technology[88], as described in previous studies[34,35,89]. $Y_2O_3$, $BaCO_3$, CuO were used as initial components for growing the crystals. However, the use of $BaCO_3$ requires preliminary high-temperature annealing of the stock for decarbonization of barium carbonate. To dope the Y sites with Pr, the $Pr_5O_{11}$ was added to the initial stock in an appropriate percentage. The regimes of growing and saturating crystals with oxygen were the same as described elsewhere[34,35,90].

Rectangular crystals of about $3 \times 0.5 \times 0.3$ mm$^3$ (0.3 mm corresponds to the c-axis) were chosen from the same batch for the resistivity measurements. Samples with unidirectional twin boundaries were obtained and a bridge ~0.2 mm wide and with 0.3 mm spacing between pairs of electrical contacts was cut from the crystal. In

this case, the experimental geometry was chosen in such a way that the vector of the transport current I along the bridge was parallel to the twinning planes (I || TB)[12,35,91]. An automated setup engulfing the four-point probe technique (here stabilized measuring current of up to 10 mA) was employed to determine the ab-plane resistivity, $\rho_{ab}(T)$[46,92]. The silver epoxy contacts were glued to the end points of the crystal aiming to form a uniform current distribution in the central region where voltage probes in the form of parallel stripes were placed. Contact resistances below 1 Ω were obtained.

The sample morphology, the arrangement of contacts and other details are discussed in previous work[29,46]. Temperature measurements were performed with a platinum sensor with an accuracy of about 1 mK. The hydrostatic P was generated inside a Teflon cup in a copper–beryllium piston-cylinder cell, as described in previous work[93]. The applied pressure was measured using a manganin gauge made of a 25 Ω wire. Transformer oil acted as the transmitting medium and pressures were changed at room temperature in the order of increasing magnitude. At every P, experimental measurements were performed at rates of about 0.1 K/min near $T_c$ and 0.5 K/min at $T \gg T_c$.

Received: 30 July 2019; Accepted: 30 November 2019;
Published online: 31 December 2019

## References

1. Robinson, N. J., Johnson, P. D., Rice, T. M. & Tsvelik, A. M. Anomalies in the pseudogap phase of the cuprates: Competing ground states and the role of umklapp scattering. *Rep. Prog. Phys.* **82** 126501 https://doi.org/10.1088/1361-6633/ab31ed (2019).
2. Kivelson, S. A. & Lederer S. Linking the pseudo-gap in the cuprates with local symmetry breaking: a commentary. *PNAS* **116**, 14395–14397 https://doi.org/10.1073/pnas.1908786116 (2019).
3. Mishra, V., Chatterjee, U., Campuzano, J. C. & Norman, M. R. Effect of the pseudogap on the transition temperature in the cuprates and implications for its origin. *Nat. Phys.* **10**, 357–360 (2014).
4. Peters, R. & Bauer, J. Local origin of the pseudogap in the attractive Hubbard model. *Phys. Rev. B* **92**, 014511–014513 (2015).
5. Emery, V. J. & Kivelson, S. A. Importance of phase fluctuations in superconductors with small superfluid density. *Nature (London)* **374**, 434–437 (1995).
6. Randeria, M. Ultracold Fermi gases: Pre-pairing for condensation. *Nat. Phys.* **6**, 561–562 (2010).
7. Badoux, S. *et al.* Change of carrier density at the pseudogap critical point of a cuprate superconductor. *Nature (London)* **531**, 210–214 (2016).
8. Rullier-Albenque, F., Alloul, H. & Rikken, G. High-field studies of superconducting fluctuations in high-$T_c$ cuprates: Evidence for a small gap distinct from the large pseudogap. *Phys. Rev. B* **84**, 014522–014544 (2011).
9. Kordyuk, A. A. Pseudogap from ARPES experiment: three gaps in cuprates and topological superconductivity. *Low Temp. Phys.* **41**, 417–444 (2015).
10. Seibold, G. *et al.* Marginal Fermi Liquid behaviour from charge density fuctuations in cuprates. arXiv:1905.10232v1 (2019).
11. Esterlis, I., Kivelson, S. A. & Scalapin, D. J. Pseudogap crossover in the electron-phonon system. *Phys. Rev. B* **99**, 174516 (2019).
12. Vovk, R. V. & Solovjov, A. L. Electric transport and pseudogap in high-temperature superconducting compounds of system 1-2-3 under conditions of all-round compression. *Low Temp. Phys.* **44**, 111–153 (2018).
13. Physical Properties High Temperature Superconductors I, D. M. Ginsberg (ed.), Word Scientific, Singapore (1989).
14. Matsuda, Y. *et al.* Magnetoresistance of *c*-axis-oriented epitaxial $YBa_2Cu_3O_{7-x}$ films above $T_c$. *Phys. Rev. B* **40**, 5176–5179 (1989).
15. Triscone, J.-M. *et al.* $YBa_2Cu_3O_7/PrBa_2Cu_3O_7$ superlattices: Properties of Ultrathin superconducting layers separated by insulating layers. *Phys. Rev. Lett.* **64**, 804 (1990).
16. Jia, Y. X., Liu, J. Z., Lan, M. D. & Shelton, R. N. Hall effect in the mixed state of $Y_{1-x}Pr_xBa_2Cu_3O_{7-\delta}$ single crystals. *Phys. Rev. B* **47**, 6043 (1993).
17. Vovk, R. V., Nazyrov, Z. F., Goulatis, I. L. & Chroneos, A. Metal-to-insulator transition in $Y_{1-x}Pr_xBa_2Cu_3O_{7-\delta}$ single crystals with various praseodymium contents. *Physica C* **485**, 89–91 (2013).
18. Solovjov, A. L. & Dmitriev, V. M. Fluctuation conductivity and pseudogap in $Y_{1-x}Pr_xBa_2Cu_3O_{7-y}$ films. *Low Temp. Phys.* **32**, 576–581 (2006).
19. Fehrenbacher, R. & Rice, T. M. Unusual electronic structure of $PrBa_2Cu_3O_7$. *Phys. Rev. Lett.* **70**, 3471 (1993).
20. Yu, Y., Cao, G. & Jiao, Z. Hole distribution and Tc suppression in $Y_{1-x}Pr_xBa_2Cu_3O_7$. *Phys. Rev. B* **59**, 3845 (1999).
21. Nagasawa, H. & Sugawara, T. The Magnetism of Praseodymium Metal. *J. Phys. Soc. Jpn.* **23**, 701–710 (1967).
22. Guillaume, M. P. *et al.* Magnetic order of Pr ions in related perovskite-type Pr123 compounds. *J. Appl. Phys.* **75**, 6331 (1994).
23. Solovjov, A. L. *et al.* Specific temperature dependence of pseudogap in $YBa_2Cu_3O_{7-\delta}$ nanolayers. *Phys. Rev. B* **94**, 224505 (2016).
24. Solovjov, A. L. *et al.* Pseudogap and fluctuation conductivity in $Y_{1-x}Pr_xBa_2Cu_3O_{7-\delta}$ single crystals with different concentrations of praseodymium. *Low Temp. Phys.* **43**, 841 (2017).
25. Liu, H. J. *et al.* Hydrostatic-pressure effects on the a-axis resistance of monocrystalline $Bi_{2.2}(Sr,Ca)_{2.8}Cu_2O_{8+y}$. *Phys. Rev. B* **51**, 9167 (1995).
26. Wang, Q. *et al.* Electrical resistance under pressure in textured $Bi_2Sr_2CaCu_2O_{8+y}$: Enhancement of the energy gap and thermodynamic fluctuations. *Phys. Rev. B* **55**, 8529 (1997).
27. Ferreira, L. M. *et al.* Effects of pressure on the fluctuation conductivity of $YBa_2Cu_3O_7$. *Phys. Rev. B* **69**, 212505 (2004).
28. Huang, H. *et al.* Modification of structural disorder by hydrostatic pressure in the superconducting cuprate $YBa_2Cu_3O_{6.73}$. *Phys. Rev. B* **97**, 174508 (2018).
29. Vovk, R. V. *et al.* Phase separation in oxygen deficient $HoBa_2Cu_3O_{7-\delta}$ single crystals: effect of high pressure and twin boundaries. *Philos. Mag.* **91**, 2291–2302 (2011).
30. Vovk, R. V. *et al.* Effect of long aging on the resistivity properties of optimally doped $YBa_2Cu_3O_{7-\delta}$ single crystals. *Solid State Commun.* **170**, 6–9 (2013).
31. Maisuradze, A. *et al.* Muon spin rotation investigation of the pressure effect on the magnetic penetration depth in $YBa_2Cu_3O_x$. *Phys. Rev. B* **84,**, 184523 (2011).
32. Akhavan, M. The question of Pr in HTSC. *Physica B* **321**, 265–282 (2002).
33. Lacayo, G., Kastner, G. & Hermann, R. Twin to tweed transition in $YBa_2Cu_3O_{7-\delta}$ by substitution of Al for Cu. *Physica C* **192**, 207–214 (1992).
34. Vovk, R. V. *et al.* Incoherent transport and pseudogap in $HoBa_2Cu_3O_{7-\delta}$single crystals with different oxygen content. *J. Mater. Sci.: Mater. Electron.* **20**, 858–860 (2009).
35. Vovk, R. V. *et al.* Electro-transport and structure of 1-2-3 HTSC single crystals with different plane defects topologies. *J. Mater Sci.: Mater. Electron.* **23**, 1255–1259 (2012).
36. Vovk, R. V. *et al. c*-axis hopping conductivity in heavily Pr-doped YBCO single crystals. *Supercond. Sci. Technol.* **26**, 085017 (2013).

37. Fang, Y., Yazici, D., White, B. D. & Maple, M. B. Pressure-induced phase transition in $La_{1-x}Sm_xO_{0.5}F_{0.5}BiS_2$. *Phys. Rev. B* **92**, 094507 (2015).
38. Solovjov, A. L. *et al*. Hydrostatic-pressure effects on the pseudogap in slightly doped $YBa_2Cu_3O_{7-\delta}$ single crystals. *Physica B: Condenced Matter* **493**, 58–67 (2016).
39. Solovjov, A. L. *et al*. Peculiarities in the pseudogap behavior in optimally doped $YBa_2Cu_3O_{7-\delta}$ single crystals under pressure up to 1 GPa. *Curr. Appl. Phys.* **16**, 931–938 (2016).
40. Vovk, R. V. *et al*. Relaxation of the normal electrical resistivity induced by high-pressure in strongly underdoped $YBa_2Cu_3O_{7-\delta}$ single crystals. *Physica B* **407**, 4470–4472 (2012).
41. Alloul, H., Rullier-Albenque, F., Vignolle, B., Colson, D. & Forget, A. Superconducting fluctuations, pseudogap and phase diagram in cuprates. *EPL* **91**, 37005–37010 (2010).
42. Lang, W. *et al*. Paraconductivity and excess Hall effect in epitaxial $YBa_2Cu_3O_7$ films induced by superconducting fluctuations. *Phys. Rev. B* **49**, 4209 (1994).
43. Ando, Y. *et al*. Electronic phase diagram of high-$T_c$ cuprate superconductors from a mapping of the in-plane resistivity curvature. *Phys. Rev. Lett.* **93**, 267001 (2004).
44. Solovjov, A. L., Habermeier, H.-U. & Haage, T. Fluctuation conductivity in $YBa_2Cu_3O_{7-y}$ films of various oxygen content. II. YBCO films with $T_c$»80 K. *Low Temp. Phys.* **28**, 144–156 (2002).
45. L. de Mello, E. V. *et al*. Pressure studies on the pseudogap and critical temperatures of a high-Tc superconductor. *Phys. Rev. B* **66**, 092504 (2002).
46. Solovjov, A. L., Tkachenko, M. A., Vovk, R. V. & Chroneos, A. Fluctuation conductivity and pseudogap in HoBaCuO single crystals under pressure with transport current flowing under an angle 45° to the twin boundaries. *Physica C* **501**, 24–31 (2014).
47. Gupta, R. & Gupta, M. Relationship between pressure-induced charge transfer and the superconducting transition temperature in $YBa_2Cu_3O_{7-\delta}$ superconductors. *Phys. Rev. B* **51**, 11760 (1995).
48. Shen, L. J. *et al*. Thermodynamic fluctuation under high pressure in Hg-1223 superconductors. *Supercond. Sci. Technol.* **11**, 1277 (1998).
49. Neumeier, J. J. & Zimmermann, H. A. Pressure dependence of the superconducting transition temperature of $YBa_2Cu_3O_7$ as a function of carrier concentration: A test for a simple charge-transfer model. *Phys. Rev. B* **47**, 8385 (1993).
50. Gvozdicov, V. M. Van Hove singularity and anomalous shift of the superconducting transition in untwinned $YBa_2Cu_3O_{7-\delta}$ under uniaxial pressure. *Physica C* **235–240**, 2127 (1994).
51. Perali, A. & Varelogiannis, G. Anisotropic pressure dependence of the critical temperature in $YBa_2Cu_3O_7$. *Phys. Rev. B* **61**, 3672 (2000).
52. Welp, U. *et al*. Effect of uniaxial stress on the superconducting transition in $YBa_2Cu_3O_7$. *Phys. Rev. Lett.* **69**, 2130 (1992).
53. Schwingensclogl, U. & Schuster, C. Doping and defects in $YBa_2Cu_3O_7$: Results from hybrid density functional theory. *Appl. Phys. Lett.* **100**, 253111 (2012).
54. Prokof'ev, D. D., Volkov, M. P. & Bojkov, Y. A. Pseudogap and its temperature dependence in YBCO from the data of resistance measurements. *Phys. Solid State* **45**, 1223–1232 (2003).
55. Stojkovic, B. P. & Pines, D. Theory of the longitudinal and Hall conductivities of the cuprate superconductors. *Phys. Rev. B* **55**, 8576 (1997).
56. Taillefer, L. Scattering and Pairing in Cuprate Superconductors. *Annu. Rev. Condens. Matter Phys.* **1**, 51–70 (2010).
57. Timusk, T. & Statt, B. The pseudogap in high-temperature superconductors: an experimental survey. *Rep. Prog. Phys.* **62**, 161–222 (1999).
58. Alloul, H., Ohno, T. & Mendels, P. $^{89}Y$ NMR evidence for a fermi-liquid behavior in $YBa_2Cu_3O_{6+x}$. *Phys. Rev. Lett.* **63**, 1700–1703 (1989).
59. Kondo, T. *et al*. Formation of Gapless Fermi Arcs and Fingerprints of Order in the Pseudogap State of Cuprate Superconductors. *Phys. Rev. Lett.* **111**, 157003 (2013).
60. Solovjov, A. L. Superconductors - Materials, Properties and Applications. Chapter 7: Pseudogap and local pairs in high-Tc supeconductors, - A. M. Gabovich (ed.).- InTech: Rijeka, **7**, 137 (2012).
61. Solovjov, A. L. & Dmitriev, V. M. Resistive studies of the pseudogaps in YBCO films with consideration of the transition from BCS to Bose-Einstein condensation. *Low Temp. Phys.* **32**, 99–108 (2006).
62. Oh, B. *et al*. Upper critical field, fluctuation conductivity, and dimensionality of $YBa_2Cu_3O_{7-x}$. *Phys. Rev. B* **37**, 7861 (1988).
63. De Gennes, P. G. *Superconductivity of Metals and Alloys* (W. A. Benjamin, Inc., New York, Amsterdam) **280** (1968).
64. Chryssikos, G. D. X-ray diffraction and infrared investigation of $RBa_2Cu_3O_7$ and $R_{0.5}Pr_{0.5}Ba_2Cu_3O_7$ compounds (R-Y and lanthanides). *Physica C* **254**, 44–62 (1995).
65. Aslamazov, L. G. & Larkin, A. L. The influence of fluctuation pairing of electrons on the conductivity of the normal metal. *Phys. Lett. A* **26**, 238–239 (1968).
66. Kapitulnik, A., Beasley, M. R., Castellani, C. & DiCastro, C. Thermodynamic fluctuations in the high-$T_c$ perovskite superconductors. *Phys.Rev. B* **37**, 537 (1988).
67. Hikami, S. & Larkin, A. I. Magnetoresistance of high temperature superconductors. *Mod. Phys. Lett. B* **2**, 693–698 (1988).
68. Solovjov, A. L. Fluctuation conductivity in Y-Ba-Cu-O films with artificially produced defects. *Low Temp. Phys.* **28**, 1138–1149 (2002).
69. Caprara, S., Grilli, M., Leridon, B. & Lesueur, J. Extended paraconductivity regime in underdoped cuprates. *Phys. Rev. B* **72**, 104509 (2005).
70. Caprara, S., Grilli, M., Leridon, B. & Vanacken, J. Paraconductivity in layered cuprates behaves as if due to pairing of nearly free quasiparticles. *Phys. Rev. B* **79**, 024506 (2009).
71. Xie, Y. B. Superconducting fluctuations in the high-temperature superconductors: Theory of the dc resistivity in the normal state. *Phys. Rev. B* **46**, 13997–14000 (1992).
72. Leridon, B., Défossez, A., Dumont, J., Lesueur, J. & Contour, J. P. Conductivity of Underdoped $YBa_2Cu_3O_{7-\delta}$: Evidence for incoherent pair correlations in the pseudogap regime. *Phys. Rev. Lett.* **87**, 197007 (2001).
73. Leridon, B. *et al*. Evidence for Pairing Correlations in the Pseudogap State of Underdoped High-*Tc* Cuprates Thin Films. *Journal of Superconductivity: Incorporating Novel Magnetism* **15**, 409–412 (2002).
74. Ludwig, H. A. *et al*. X-ray investigations of $Y_1Ba_2Cu_4O_8$ under high pressure. *Physica, C* **167**, 335–338 (1990).
75. Corson, J. R. Vanishing of phase coherence in underdoped $Bi_2Sr_2CaCu_2O_{8+\delta}$. *Nature* **398**, 221–223 (1999).
76. Kawabata, K. *et al*. Detection of a coherent boson current in the normal state of a high-temperature superconductor $YBa_2Cu_3O_y$ film patterned to micrometer-sized rings. *Phys. Rev. B* **58**, 2458–2461 (1998).
77. Stajic, E. *et al*. Cuprate pseudogap: Competing order parameters or precursor superconductivity. *Phys. Rev. B* **68**, 024520–024529 (2003).
78. Yamada, Y. *et al*. Interlayer tunneling spectroscopy and doping-dependent energy-gap structure of the trilayer superconductor $Bi_2Sr_2Ca_2Cu_3O_{10+\delta}$. *Phys. Rev. B* **68**, 054533 (2003).
79. Zaitsev, R. O. Peculiarities of the electron mechanism of superconductivity. *JETP* **98**, 780–792 (2004).
80. Wang, K. W. & Ching, W. Y. A structural-based microscopic theory on high-temperature cuprate superconductors. *Physica C* **416**, 47–67 (2004).

81. D'yachenko, A. I. & Tarenkov, V. Yu. Effects of pressure on the spectroscopic characteristics of Bi2223 cuprates. *Phys. Tech. High. Press.* **24**, 24–42 (2014).
82. Solovjov, A. L. & Dmitriev, V. M. Electric transport and Hall effect in $Y_{1-x}PrxBa_2Cu_3O_{7-y}$ films. *Low Temp. Phys.* **33**, 32–40 (2007).
83. Solovjov, A. L. & Dmitriev, V. M. Fluctuation conductivity and pseudogap in high-temperature YBCO superconductors. *Low Temp. Phys.* **35**, 169–197 (2009).
84. Haussmann, R. Properties of a Fermi liquid at the superfluid transition in the crossover region between BCS superconductivity and Bose-Einstein condensation. *Phys. Rev. B* **49**, 12975 (1994).
85. Engelbrecht, J. R. Pseudogap above Tc in a model with dx2 − y2 pairing. *Phys. Rev. B* **57**, 13406 (1998).
86. Schneider, T. & Singer, J. M. Phase Transition Approach to High Temperature Superconductivity: Universal Properties of Cuprate Superconductors. Imperial College Press, London, (2000).
87. Peng, Y. Y. *et al*. Re-entrant charge order in overdoped $(Bi, Pb)_{2.12}Sr_{1.88}CuO_{6+\delta}$ outside the pseudogap regime. *Nature Materials* **17**, 697–702 (2018).
88. Ono, A. & Tanaka, T. Preparation of Single Crystals of the Superconductor $Ba_2YCu_3O_{6.5+x}$. *Jpn. J. Appl. Phys.* **26**, 825 (1987).
89. Moshchalkov, V. V. *et al*. Superconductivity and localization in $YBa_2Cu_3O_x$ oxides. *Low Temp. Phys.* **14**, 988–991 (1988).
90. Vovk, R. V. *et al*. Scattering Processes of Normal and Fluctuating Carriers in $ReBa_2Cu_3O_{7-\delta}$ (Re = Y, Ho) Single Crystals with Unidirectional Twin Boundaries. *Acta Physica Polonica A* **111**, 123–128 (2007).
91. Khadzhai, G. Y. *et al*. The effect of high pressure on critical temperature of $Y_{0.95}Pr_{0.05}Ba_2Cu_3O_{7-\delta}$ single crystals with a given topology of planar defects. *Low Temp. Phys.* **40**, 900–903 (2014).
92. Vovk, R. V. *et al*. Effect of high pressure on the fluctuation conductivity and the charge transfer of $YBa_2Cu_3O_{7-\delta}$ single crystals. *J.Alloys Compd.* **453**, 69–74 (2008).
93. Thompson, J. D. Low - temperature pressure variations in a self - clamping pressure cell. *Rev. Sci. Instrum.* **55**, 231 (1984).


## Author contributions

The experiments were performed by A.L.S. All the authors discussed and analyzed the results and contributed to the writing of the paper.

## Competing interests

The authors declare no competing interests.

## Additional information

**Correspondence** and requests for materials should be addressed to A.C.

**Reprints and permissions information** is available at www.nature.com/reprints.

**Publisher's note** Springer Nature remains neutral with regard to jurisdictional claims in published maps and institutional affiliations.